Image reconstruction of a perfectly conducting cylinder by the genetic algorithm

C.-C. Chiu
P.-T. Liu

Abstract: The paper presents a computational approach to reconstruct the shape of a perfectly conducting cylinder. Based on the boundary condition and the measured scattered field, a set of nonlinear integral equations is derived and the imaging problem is reformulated into an optimum one. By using the genetic algorithm, the shape of the object can be reconstructed. The genetic algorithm will always converge to a global extreme solution no matter what the initial estimate. Numerical results are given to demonstrate that, even when the initial guess is far away from the exact one, good reconstruction has been obtained. In such a case, the calculus-based method often becomes trapped in a local extreme.

1 Introduction

Inverse scattering of conducting objects has been a subject of considerable importance in various areas of technology. Two categories of approaches have generally been developed. The first is an approximate approach which makes use of the Bojarski identity to reconstruct the shape of a perfectly conducting scatterer [1–5]. However, this method requires a physical-optics approximation. In contrast, the second approach is to solve the exact equations rigorously by numerical methods [6–13]. The rigorous method needs no approximation in formulation, but the nonlinearity and illposedness are more serious than for the approximate method. As a result, many inverse problems are reformulated as optimisation problems. There are two main different forms of cost functional for such optimisation. The first form of the cost functional is intuitively defined as the root-mean-square error between the calculated scattered field and the measured scattered field [6–9]. A solution which satisfies the boundary condition can be found by searching the minimum of the cost functional. The second form of the cost functional consists of two terms: one term is the same as the cost functional defined in the first form; the other is the

root-mean-square error in satisfying the boundary integral equation [10–13]. Note that *a priori* information or regularisation terms can be added in the above two cost functionals to overcome illposedness. The two optimisation schemes are numerical solved by different iterative methods such as Newton–Kantorovitch method [6–8], Levenberg–Marquardt algorithm [10–12] and conjugate-gradient method [13]. However, the above mentioned rigorous approaches almost apply the calculus-based method to find the extreme by setting the gradient of the objective function equal to zero at each iteration. This method often becomes trapped in a local extreme, when the initial guess is far from the exact one.

The current literature identifies three main types of search method: calculus-based, enumerative, and random methods [14]. The genetic algorithm is a well known algorithm which uses random choice to search through a coding of a parameter space. This algorithm has achieved increasing popularity as researchers have recognised the shortcomings of calculus-based and enumerative schemes. Theoretically, the genetic algorithm and enumerative method converge to the global extreme of the problem, while calculus-based method often becomes trapped in a local extreme. On the other hand, the enumerative scheme lacks efficiency compared with the other two methods. As a result, the genetic algorithm is the most robust scheme among the three methods. Unfortunately, few papers have applied the genetic algorithm to solve the inverse problem [15].

In this paper, we present a method based on the genetic algorithm to recover the shape of an impenetrable cylinder.

2 Theoretical formulation

2.1 Direct problem

Let us consider a perfectly conducting cylinder located in a free space and let (ε_0, μ_0) denote the permittivity and permeability of the free space, respectively. The metallic cylinder with cross-section described in polar co-ordinates in the xy plane by the equation $\rho = F(\theta)$ is illuminated by an incident plane wave whose electric-field vector is parallel to the z axis (i.e. transverse magnetic or TM polarisation). We assume that the time dependence of the field is harmonic with the factor $\exp(j\omega t)$. Let $\mathbf{E}_i$ denote the incident field with incident angle ϕ, as shown in Fig. 1. Then the incident field is given by

$$\mathbf{E}_i(\mathbf{r}) = \exp\{-jk(x\sin\phi + y\cos\phi)\hat{z}, \quad k^2 = \omega^2\varepsilon_0\mu_0 \quad (1)$$

IEE Proc.-Microw. Antennas Propag., Vol. 143, No. 3, June 1996

249

At an arbitrary point (x, y) in cartesian co-ordinates or (r, θ) in polar co-ordinates outside the scatterer, the scattered field $E_s = E - E_i$, can be expressed by

$$E_s(x, y) =$$

$$-\int_0^{2\pi} \frac{j}{4} H_0^{(2)} \left(k\sqrt{\{x-F(\theta')\cos(\theta')\}^2 + \{y-F(\theta')\sin(\theta')\}^2} \right) J(\theta') d\theta'$$

(2)

with

$$J(\theta) = -j\omega\mu_0 \sqrt{F^2(\theta) + F'^2(\theta)} J_s(\theta)$$

where $H_0^{(2)}$ is the Hankel function of the second of order zero, and $J_s(\theta)$ is the induced surface current density which is proportional to the normal derivative of electric field on the conductor surface. Note that the scattered field for large values of r in eqn. 2 can be expressed in asymptotic form as

$$E_s(x, y) \sim \frac{\exp(-jkr)}{\sqrt{r}} G_s(\theta)$$

$$G_s(\theta) = -\frac{j}{4} \left(\sqrt{\frac{2}{\pi k}} \right) \exp(j\pi/4)$$

$$\times \int_0^{2\pi} \exp\{jkF(\theta')\cos(\theta - \theta')\} J(\theta') d(\theta')$$

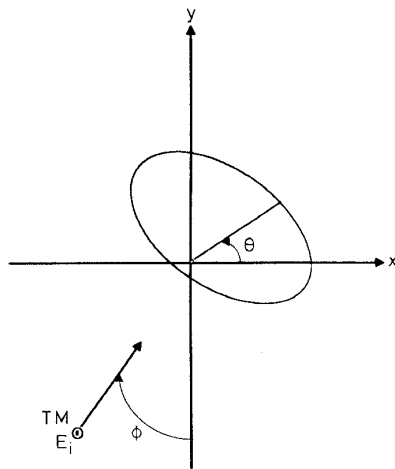where $G_s(\theta)$ is known as the scattered far-field pattern.

Fig. 1 Geometry of problem in (x, y) plane

The boundary condition at the surface of the scatterer states that the total tangential electric field must be zero and this yields an integral equation for $J(\theta)$:

$$E_i\{F(\theta), \theta\} = \int_0^{2\pi} \frac{j}{4} H_0^{(2)}(kr_o) J(\theta') d\theta'$$

(3)

where

$$r_0(\theta, \theta') = \{F^2(\theta) + F^2(\theta') - 2F(\theta)F(\theta')\cos(\theta - \theta')\}^{1/2}$$

For the direct-scattering problem, the scattered field E_s is calculated by assuming that the shape of the object is known. This can be achieved by first solving J in eqn. 3 and calculating E_s in eqn. 2. For numerical calculation of the direct problem, the contour is first divided into sufficient small segments so that the induced surface

current can be considered constant over each segment. Then the moment method [16] is used to solve eqns. 3 and 2 with a pulse basis function for expanding and the Dirac delta function for testing.

2.2 Genetic algorithm

The genetic algorithm is a search algorithm based on the mechanics of natural selection and natural genetics. This algorithm has achieved increasing popularity as researchers have recognised the shortcoming of calculus-based and enumerative schemes. They find the global maximum of an objective function (or fitness function) of the problem by random search. The natural parameter set of the optimisation problem is first coded as a finite-length string. Then three operators — reproduction, crossover and mutation — are employed to search the optimisation of the problem through a coding of a parameter space. Reproduction is a process in which individual strings are copied according to their objective-function value. Intuitively, we can think of the object function as some measure of profit, utility or goodness that we want to maximise. Copying strings according to their fitness values means that strings with a higher value have a higher probability of contributing one or more offspring in the next generation. After reproduction, simple crossover may proceed in two steps. First, members of the newly reproduced strings in the mating pooling are mated at random. Secondly, each selected pair of strings undergoes crossing over and then produces two new strings. Each bit value of the two new strings is chosen randomly from that of the two selected strings on the same bit position. After crossover, mutation operation is applied. Mutation is the occasional (with small probability) random alteration of the bit value of a string. In the binary coding of the parameter, this simply means changing a 1 to 0 and vice versa. The above three operations have proved to be both computationally simple and effective in attacking a number of important optimisation problems. The flow chart for the genetic algorithm is shown in Fig. 2.
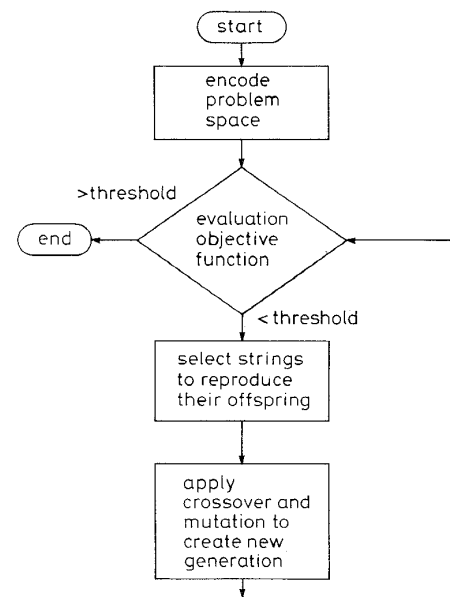

Fig. 2 Flowchart of the genetic algorithm

2.3 Inverse problem

We consider the following problem. Given the scattered field E_s measured outside the scatterer, determine the shape $F(\theta)$ of the object. For numerical calculation of the inverse problem, we choose the following expansions:

$$F(\theta) = \sum_{n=0}^{N/2} A_n \cos(n\theta) + \sum_{n=1}^{N/2} A'_n \sin(n\theta) \qquad (4)$$

where A_n and A'_n are real numbers and $N + 1$ is the number of unknowns. Note that the discretisation number of $J(\theta)$ for the inverse problem must be different from that for the direct problem. In our simulation, the discretisation number for the direct problem is twice that for the inverse problem. Since it is crucial that the synthetic data generated through a direct solver are not like those obtained by the inverse solver, in the inversion procedure, the genetic algorithm is used to maximise the objective function

$$SF = \left\{ \frac{1}{M_t} \sum_{m=1}^{M_t} |E_s^{exp}(\mathbf{r}_m) - E_s^{cal}(\mathbf{r}_m)|^2 / |E_s^{exp}(\mathbf{r}_m)|^2 + \alpha |F'(\theta)|^2 \right\}^{-1/2}$$

$$(5)$$

where M_t is the total number of measurement points. $E_s^{cal}(\mathbf{r})$ and $E_s^{exp}(\mathbf{r})$ are the calculated scattered field and the measured scattered field, respectively. Note that the regularisation term $\alpha |F'(\theta)|2$ has been added in eqn. 5, where typical values of α range from 0.0001 to 10. The optimal value of α depends mainly on the dimensions of the geometry. In applying the genetic algorithm, the maximum string length is chosen first; then the unknown coefficient of the shape function is coded as a population of strings. Here, physical constraints are used to limit the extreme value of the coefficients of shape function. A random start using successive coin flips (head = 1, tail = 0) generates the initial population. The genetic algorithm starts with this population of strings and thereafter generates successive populations of strings by employing reproduction, crossover and mutation operations. The generation process will be stopped when either SF changes by less than 1% SF is larger then 10^5 in two successive generations.

3 Numerical results

By numerical simulation, we illustrate the performance of the proposed inversion algorithm and its sensitivity to random error in the scattered field. Let us consider a perfectly conducting cylinder in a free space and a plane wave of unit amplitude incident on the object, as shown in Fig. 1. The frequency of the incident wave is chosen to be 300MHz, i.e. the wavelength λ is 1m.

In our calculation four examples are considered. To reconstruct the shape of the cylinder, the object is illuminated by the four incident waves with incident angles $\phi = 0°$, $90°$, $180°$ and $270°$, and the measurement is taken on a circle of radius R' at equal spacing. In our case, R' is chosen to be 10m corresponding to the far-field measurement. Note that for each incident angle eight measurement points at equal spacing are used, and there are 32 measurement points in all in each simulation. The number of unknowns is set to be nine (i.e. $N + 1 = 9$). Population size is chosen as 300. The crossover probability and mutation probability are set to be 0.8 and 0.04, respectively. The value of α is 0.001. The length of coding is set to be eight bits and the search

range for the unknown coefficient of the shape function is chosen from 0 to 2 for the first three examples. In the fourth example, the length of coding is 10 bits and the search range is from 0 to 8.

We now report on four different shape functions we have computed. Note that the reconstructed result of the last generation in each example is not plotted since it cannot be distinguished from the exact result by the naked eye.
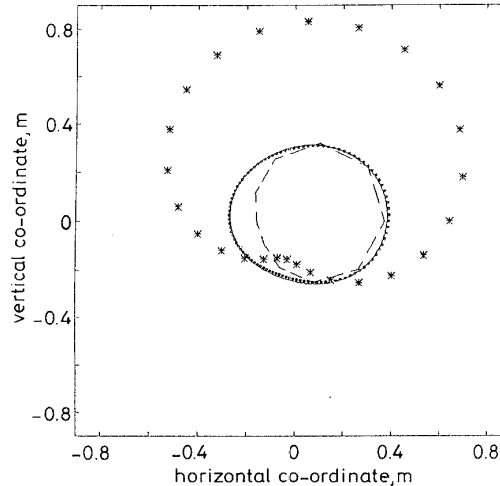

Fig.3 *Reconstructed shape function*
———— exact
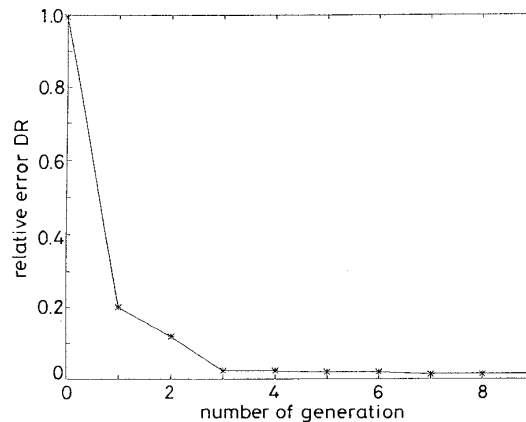****** initial
– – – – gen = 1
·········· gen = 4

Fig.4 *Error in reconstructed shape function*

In the first example, the shape function is chosen to be $F(\theta) = (0.3 + 0.06\cos\theta + 0.03\sin\theta + 0.025\cos2\theta)$ metres, the reconstructed shape function is plotted in Fig. 3 with the error shown in Fig. 4. Here DR, which is called shape function discrepancies, is defined as

$$DR = \left[\frac{1}{N'} \sum_{i=1}^{N'} \left\{ F^{cal}(\theta_i) - F(\theta_i) \right\}^2 / F^2(\theta_i) \right]^{1/2} \qquad (6)$$

where N' is set to be 60. The quantities DR provide measures of how well $F^{cal}(\theta)$ approximates $F(\theta)$. From Figs. 3 and 4, is clear that the reconstruction of the shape function is fairly good. Note that the shape function of the initial generation is far from the exact one. The typical CPU time for the example is about 30 min on a Sun Sparc 20.

IEE Proc.-Microw. Antennas Propag., Vol. 143, No. 3, June 1996

251

For investigating the effect of noise, we add to each complex scattered field $E_s(\mathbf{r})$ a quantity $b + cj$ where b and c are independent random numbers having a Gaussian distribution with zero mean. The standard derivation of noise is normalised by the root-mean-square value of the scattered field. The noise standard derivations applied include 10^{-4}, 10^{-3}, 10^{-2}, 10^{-1}, 2×10^{-1} and 4×10^{-1}. The numerical results are shown in Fig. 5. It shows that the effect of noise is tolerable for noise levels below 10^{-1}.
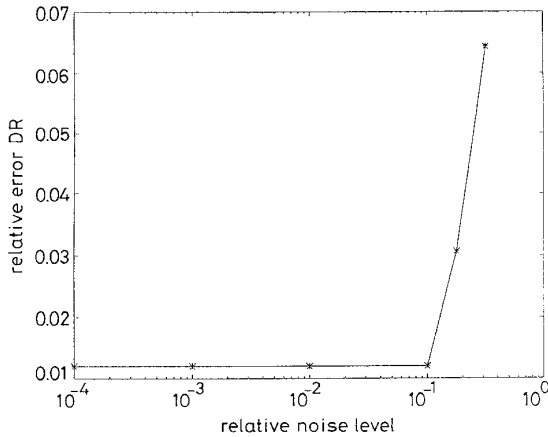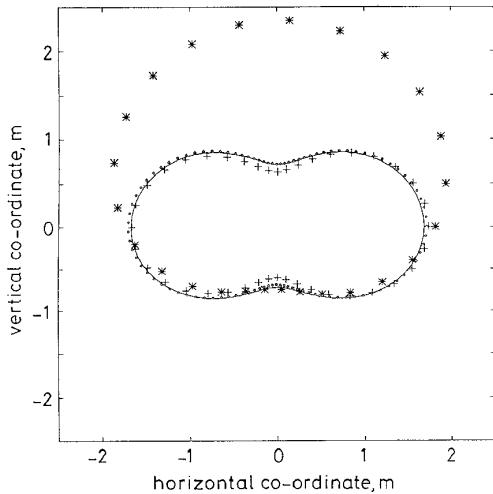

Fig.5   *Numerical results for first example*

Fig.6   *Satisfactory results for second example*
——— exact
****** initial
– – – – gen = 2
·········· gen = 5

In the second example, the shape function is chosen as $F(\theta) = (1.2 + 0.48\cos2\theta)$ metres. The purpose of this example is to show that our method is able to reconstruct the object of electrical dimension exceeding one wavelength. Satisfactory results are shown in Fig. 6 with the error shown in Fig. 7.

In the third example, the shape function is selected to be $F(\theta) = (0.3 + 0.03\cos4\theta + 0.05\sin4\theta)$ metres. Note that the shape function is not symmetrical about either the x axis or the y axis. This example has further verified the reliability of our algorithm. Refer to Figs. 8 and 9 for details.

In the fourth example, the same shape function is chosen as in example three. However, the length of
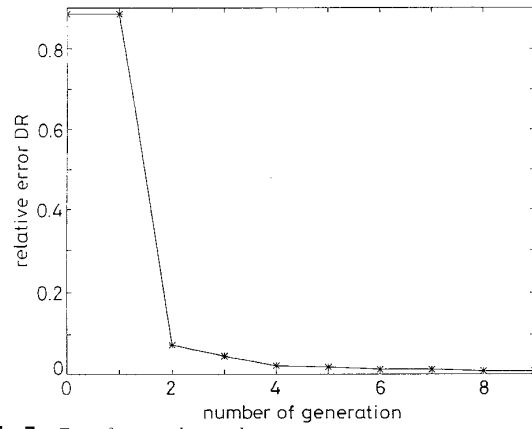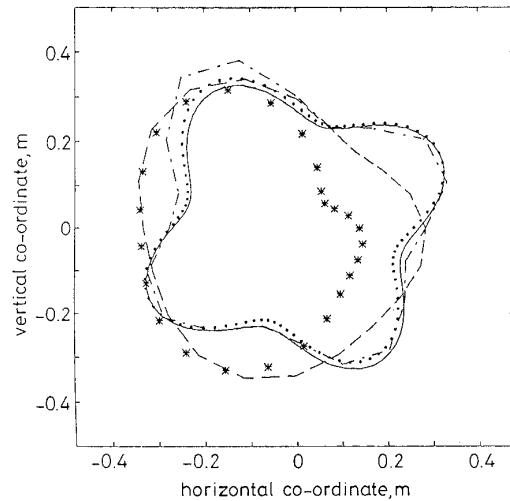

Fig.7   *Error for second example*

Fig.8   *Results for third example*
——— exact
****** initial
– – – – gen = 3
– · – · gen = 5
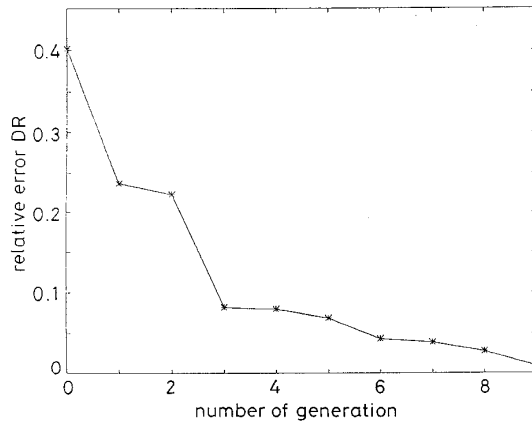·········· gen = 7

Fig.9   *Error for third example*

coding is set to be 10 bits and the search range for the unknown coefficient of the shape function is chosen from 0 to 8. The reconstructed results are shown in Fig. 10 with the error shown in Fig. 11. This example has demonstrated that, even if the search range for the unknown coefficient becomes large, good reconstruction has been obtained.
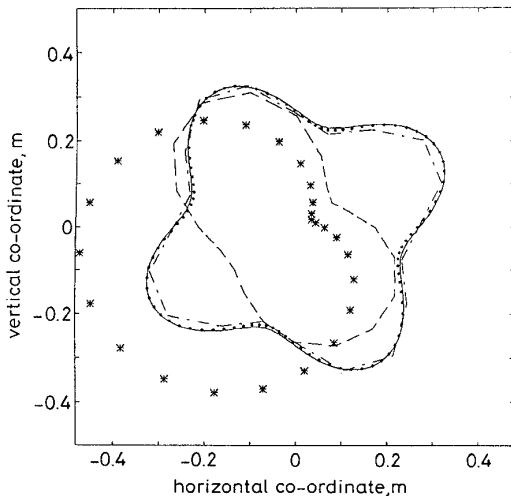
252

Fig. 10 Reconstructed results for fourth example
——— exact
✱✱✱✱✱ initial
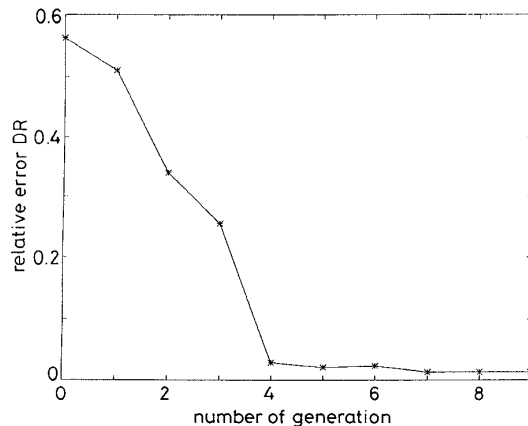– – – – gen = 3
– · – · gen = 5
·········· gen = 7

Fig. 11 Error for fourth example

4 Conclusions

We have presented a study of the application of the genetic algorithm to reconstruct the shape of a metallic object. Based on the boundary condition and the measured scattered field, a set of nonlinear integral equations is derived and reformulated into an optimum problem. The genetic algorithm is employed to find the global maximum of the objective function. Even if the initial guess is far away from the exact result, it converges to the global extreme, while the calculus-based method often becomes trapped in a local extreme.

Good reconstruction is obtained from the scattered field both with and without addition Gaussian noise. Numerical results demonstrated that the reconstruction result is still good even when the initial guess is far away from the exact result. In addition, the genetic algorithm can tackle the inverse problem for the object of electrical dimensions exceeding one wavelength. On the contrary, the calculus-based methods fail for larger scatterers. From our experience, the main difficulties in applying the genetic algorithm to this problem are how to choose the parameters, such as the bit length of the string, population size, crossover probability and mutation probability. Different parameter sets will affect the speed of convergence and the computing time required.

5 Acknowledgment

6 References

1 LEWIS, R.M.: 'Physical optics inverse diffraction', *IEEE Trans.*, 1969, **AP-17**, pp. 308–314
2 BOJARSKI, N.N.: 'A survey of the physical optics inverse scattering identity', *IEEE Trans.*, 1982, **AP-30**, pp. 980–989
3 CHU, T.H., and FARHAT, N.H.: 'Polarisation effects in microwave diversity imaging of perfectly conducting cylinders', *IEEE Trans.*, 1989, **AP-37**, pp. 235–244
4 GE, D.B.: 'A study of Lewis method for target-shape reconstruction', *Inverse Probl.*, 1990, **6**, pp. 363–370
5 CHU, T.H., and LIN, D.B.: 'Microwave diversity imaging of perfectly conducting objects in the near-field region', *IEEE Trans.*, 1991, **MTT-39**, pp. 480–487
6 ROGER, A.: 'Newton–Kantorovitch algorithm applied to an electromagnetic inverse problem', *IEEE Trans.*, 1981, **AP-29**, pp. 232–238
7 TOBOCMAN, W.: 'Inverse acoustic wave scattering in two dimensions from impenetrable targets', *Inverse Probl.*, 1989, **5**, pp. 1131–1144
8 CHIU, C.C., and KIANG, Y.M.: 'Electromagnetic imaging for an imperfectly conducting cylinder', *IEEE Trans.*, 1991, **MTT-39**, pp. 1632–1639
9 OTTO, G.P., and CHEW, W.C.: 'Microwave inverse scattering-local shape function imaging for improved resolution of strong scatterers', *IEEE Trans.*, 1994, **MTT-42**, pp. 1
10 COLTON, D., and MONK, P.: 'A novel method for solving the inverse scattering problem for time-harmonic acoustic waves in the resonance region II', *SIAM J. Appl. Math.*, 1986, **46**, pp. 506–523
11 KIRSCH, A., KRESS, R., MONK, P., and ZINN, A.: 'Two methods for solving the inverse acoustic scattering problem', *Inverse Probl.*, 1988, **4**, pp. 749–770
12 HETTLICH, F.: 'Two methods for solving an inverse conductive scattering problem', *Inverse Probl.*, 1994, **10**, pp. 375–385
13 KLEINMAN, R.E., and VAN DEN BERG, P.M.: 'Two-dimensional location and shape reconstruction', *Radio Sci.*, 1994, **29**, pp. 1157–1169
14 GOLDBERG, D.E.: 'Genetic algorithm in search, optimization and machine learning' (Addison–Wesley, 1989)
15 THOLLON, F., and BURAIS, N.: 'Geometrical optimization of sensors for eddy currents non destructive testing and evaluation', *IEEE Trans.*, 1995, **MAG-31**, pp. 2026–2031
16 HARRINGTON, R.F.: 'Field computation by moment methods' (Macmillan, 1968)